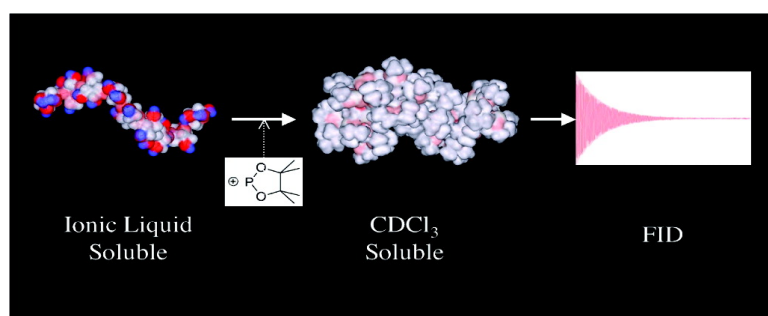Note

Hydrophobic Interactions Determining Functionalized Lignocellulose Solubility in Dialkylimidazolium Chlorides, as Probed by P NMR

Alistair W. T. King, Ilkka Kilpela#inen, Sami Heikkinen, Paula Ja#rvi, and Dimitris S. Argyropoulos

Ionic Liquid Soluble → CDCl₃ Soluble → FID

More About This Article

Additional resources and features associated with this article are available within the HTML version:

- Supporting Information
- Access to high resolution figures
- Links to articles and content related to this article
- Copyright permission to reproduce figures and/or text from this article

View the Full Text HTML

Hydrophobic Interactions Determining Functionalized Lignocellulose Solubility in Dialkylimidazolium Chlorides, as Probed by ^{31}P NMR

Alistair W. T. King,[†] Ilkka Kilpeläinen,[†] Sami Heikkinen,[†] Paula Järvi,[†] and Dimitris S. Argyropoulos*,[‡]

Laboratory of Organic Chemistry, Department of Chemistry, Faculty of Science, University of Helsinki, Helsinki, Finland, and Organic Chemistry of Wood Components Laboratories, Department of Forest Biomaterials, College of Natural Resources, North Carolina State University, Raleigh, North Carolina

Introduction

Cellulose, which is a homopolymer of β-1,4-glucose units[1] and the main constituent of wood, is the most abundant polymer on the planet and considered to be the most promising candidate for a renewable energy and materials source, potentially reducing the consumption of fossil fuels. Due to a highly regular H-bonded network between the layers of cellulose and, thus, its crystalline nature, it is quite resistant to dissolution or chemical reaction, without the use of harsh and potentially destructive conditions, if not properly controlled. Wood also contains hemicellulose, which is a carbohydrate heteropolymer, of which the monomer content can vary from different wood sources.[2] In addition to the polymeric carbohydrates, various wood sources also contain lignin, which is a noncarbohydrate heteropolymer, roughly based on seemingly random repeating units, containing a phenylpropanoid backbone, at varying degrees of oxygenation/substitution on the aromatic ring.[2] The lack of knowledge about the complex structure of lignin and its bonding interactions with other wood components has been a stumbling block for mans full utilization of wood, as a renewable resource. This is compounded by the difficulty in nondestructively fractionating the various wood components, with traditional analytical procedures being both technical and laborious. The development of future analytical procedures should require care to preserve the native structure during extraction as knowledge of the native structure is vital for designing the all important clean and efficient fractionation processes.

The assignment and quantification of individual alcoholic functionalities, in lignins such as EMAL (enzymatic mild acidolysis lignin), has been studied extensively using ^{31}P NMR, in a series of publications by Guerra and Argyropoulos et al.[3−7] It has been demonstrated that purified lignin preparations, in the absence of cellulose, can be completely dissolved in traditional organic solvents. They can then be phosphitylated, in the presence of the organic base pyridine (Pyr) and 2-chloro-4,4,5,5-tetramethyl-1,3,2-dioxaphospholane (2-Cl-TMDP) as a phosphitylating reagent, to introduce the ^{31}P label for solution-phase NMR analysis. The phosphitylated hydroxyls in lignin can then be quantitatively assessed against an internal standard
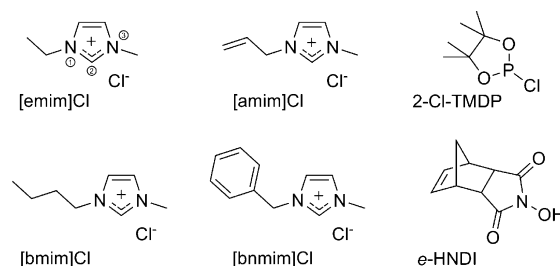

Figure 1. Structures of ILs, IS, and ^{31}P label used in this study.

(IS) such as *endo*-N-hydroxy-5-norbornene-2,3-dicarboximide (*e*-HNDI). This is the IS of choice for its adequate stability and satisfactory resolution from other lignocellulosic functionality regions, in the ^{31}P NMR spectra, after phosphitylation. To allow for quantification of hydroxyl functionalities from fully representative and potentially artifact free lignin, in minimally treated lignocellulose samples, analysis of lignin *on the fiber* is most desirable, that is, without pre-extraction of the lignin. Due to the insolubility and lack of knowledge about the reactivity of wood polysaccharides, such as cellulose, this has not been achievable under standard molecular solvent conditions.

Previously Lu and Ralph[8] have demonstrated the first reported complete dissolution of intact pulverized wood into a molecular solvent system, facilitating high resolution homogeneous solution state ^{1}H−^{13}C NMR analysis. The solvent system in question was the novel *N,N,N,N*-tetrabutylammonium fluoride-dimethylsulfoxide (TBAF-DMSO) mixture, which is now becoming a common homogeneous reaction media for cellulose functionalization.[9] The success of this and other cellulose-dissolving solvents such as the LiCl-dimethylacetamide (LiCl-DMA) mixture[1] is due to the combination of the donor properties of the high H-bond basicity from the salt anion combined with the acceptor properties of the H-bond acidity from the molecular solvent in breaking agglomerated H-bonding in the substrate. As it is our goal to develop a comprehensive ^{31}P-based method for profiling lignocellulose reactivity and quantification of functionalities in intact wood, the TBAF-DMSO solvent system would be a good starting point, however, is unsuitable for our purposes as 2-Cl-TMDP is simply too reactive for DMSO, acting as an acceptor for oxo-transfer reactions.

For almost a century, high melting organic salts such as 1-benzylpyridinium chloride ([bnPy]Cl)[10] or, more recently, molecular solvent systems such as LiCl-DMA and TBAF-DMSO,[1] containing a high content of anions with high H-bond basicity, have been shown to be capable of dissolving cellulose. Modern day ILs with melting points below 100 °C, as nonderivatizing solvents, have been demonstrated by Swatloski and Rogers et al.[11] to dissolve cellulose to varying degrees, with complete dissolution reported with 1-butyl-3-methylimidazolium chloride ([bmim]Cl), under relatively ambient conditions (<100 °C). For this study we have concentrated our efforts on the four chloride based ILs 1-allyl-3-methylimidazolium chloride ([amim]Cl), 1-benzyl-3-methylimidazolium chloride ([bnmim]Cl), [bmim]Cl, and 1-ethyl-3-methylimidazolium chloride ([emim]Cl), shown in Figure 1, to assess the effect of variation of the IL cation and not the anion in lignocellulose chemistry. Previously we have reported the tosylation and acylation of cellulose dissolved in [amim]Cl.[12] We have also extended this chemistry to pulverized wood by its complete dissolution into [amim]Cl, [bmim]Cl, or [bnmim]Cl and its subsequent functionalization

* To whom correspondence should be addressed. E-mail: dsargyro@ncsu.edu.
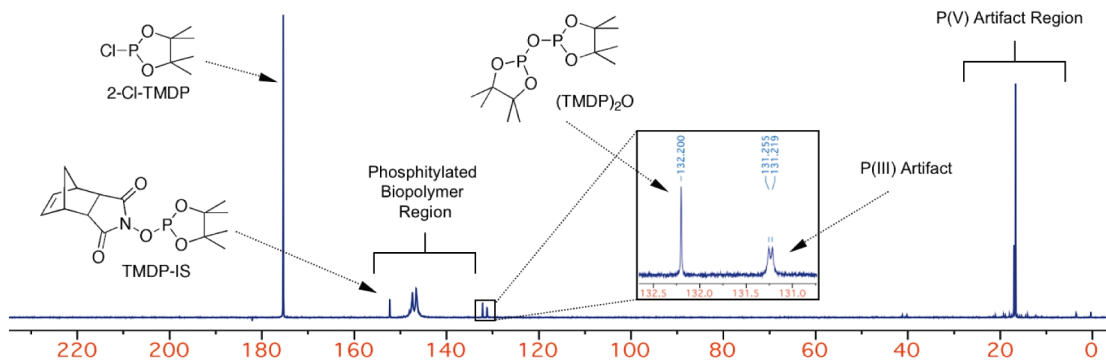† University of Helsinki.
‡ North Carolina State University.

Figure 2. Some known and unknown artifact resonances formed during the phosphitylation of MCC in [amim]Cl.

with various acyl electrophiles.[13,14] [emim]Cl was added to the above list to provide a range of ILs of varying relative hydrophobicity, imparted by the substituents on the imidazolium cation, with [emim]Cl providing the highest chloride anion content of all the possible common imidazolium chloride based ILs in the IL melting point range of 0−100 °C. In regard to the development of our analytical procedures, [amim]Cl provides us with a media that is easy to synthesize and purify, has higher chloride content, is lower melting, and has lower room temperature viscosity than other imidazolium chlorides readily available to us. The combination of the ^{31}P-labeling and NMR analysis technique with [amim]Cl, as a now common cellulose functionalization solvent,[12,15−18] allows us to directly probe the reactivity of cellulose, as the major polysaccharide biopolymer and structure of lignin as the major nonpolysaccharide biopolymer from wood in ionic liquid media, with the aim of developing a more comprehensive understanding of the various bonding interactions occurring in these solutions.

Materials and Methods

Materials. The ionic liquids [amim]Cl and [bnmim]Cl were synthesized according to a literature procedure,[12] with a few modifications in the case of [amim]Cl; prior to charcoal purification, traces of unreacted allyl chloride were removed under vacuum at 60 °C on a rotary evaporator for 5 h. After charcoal purification, the majority of the water was removed initially by rotary evaporation at 60 °C followed by slow turning at room temperature under high vacuum (1.2 mbar) for 18 h to give a pale golden oil; δ_H (300 MHz; CDCl$_3$; Me$_4$Si) 10.39 (1H, s, NCHN), 7.65 (1H, s, C=CH), 7.40 (1H, s, C=CH), 5.86 (1H, ddt, J = 16.9, 10.3, 6.5 Hz, C=CH$_2$), 5.33−5.26 (2H, m, C=CH-C), 4.86 (2H, d, J = 6.4 Hz, NCH$_2$), 3.97 (3H, s, NMe); shear viscosity (η) at 293 K was determined to be 2450 cP (lit[14] 685 cP at 303 K, lit[19] 2090 cP at 298 K); water content was initially followed by ^{1}H NMR and finally confirmed to be 0.4% by K_f titration; pH was tested by dissolving 1 g in 20 mL of deionized water to ensure neutrality. [bnmim]Cl was isolated as a clear highly viscous oil; δ_H (600 MHz; CDCl$_3$; Me$_4$Si) 10.67 (1H, s, NCHN), 7.67 (1H, s, C=CH), 7.49−7.50 (3H, m, ArH), 7.35−7.37 (3H, m, ArH), 5.59 (2H, s, PhCH$_2$N), 4.06 (3H, s, NMe); shear viscosity (η) at 313 K was determined to be 1410 cP; water content was followed by ^{1}H NMR and determined to be <1%. [bmim]Cl was purchased from Fluka. [emim]Cl was a gift from Merck. Norway Spruce EMAL was prepared according to a literature procedure.[4] Deuterated chloroform (CDCl$_3$), chromium acetylacetonate (Cr(acac)$_3$), MCC (DP = 250−300), e-HNDI, and 2-Cl-TMDP, were purchased from Aldrich Chemical Co. Viscosity measurements were recorded using a TA instruments AR2000 strain controlled rheometer, 20 mm steel plate geometry, with shear rate sweep 0.1−1000 1/s.

Typical Quantitative ^{31}P NMR Analysis of Lignocellulose Samples. The following is the typical procedure for quantitative determination of functionalities in lignocellulosic samples (MCC): Lignocellulose sample (25.0 mg) was stirred in [amim]Cl (∼0.4 mL,

475 mg) for 18 h at 80 °C in a 10 mL screw-top glass sample bottle. Pyridine (150 μL) was added in one portion and the sample was vortexed, at 2500 rpm, using a Janke & Kunkel Vibrofix VF1 Electronic orbital shaker, until visibly homogeneous (∼20 s). The sample was allowed to cool to room temperature, whereby 2-Cl-TMDP (200 μL, 1.26 mmol) was added in one portion and vortexed until visibly homogeneous (∼30 s) as a cream paste. A preprepared stock solution of Cr(acac)$_3$/CDCl$_3$ (1 mg/mL, 500 μL) was added in 4 × 125 μL portions with vortexing (∼30 s) between each addition. e-HNDI solution (121.5 mM in 3/2 pyridine/CDCl$_3$, 125 μL) was added in one portion and the solution was vortexed (∼30 s). ^{31}P NMR spectra (243 MHz) were recorded with 700 μL samples, in a 5 mm o.d. NMR tube, from this preparate and further dilutions upon Cr(acac)$_3$/CDCl$_3$ solution additions (to total volumes of 1000, 1500, 2000, 3000, and 4000 μL). For each data collection, the sample was allowed to equilibrate in the spectrometer for 5 min before the probe was retuned. Following tuning, 90° pulse widths were determined. Inverse recovery experiments were performed for most samples and optimum relaxation delay times were determined to range from 4 s at 500 μL Cr(acac)$_3$/CDCl$_3$ to 8 s at 4000 μL Cr(acac)$_3$/CDCl$_3$ for a Varian Inova 600 MHz spectrometer equipped with a direct detection probe for broadband nuclei such as ^{31}P and [13]C. CDCl$_3$ was used as locking solvent and standard transients of between 40 to 256 for 500−4000 μL Cr(acac)$_3$/CDCl$_3$ dilutions were collected for the determination of approximate phosphtylation values. Higher quality EMAL spectra were typically run overnight (12 h, 5000 transients). The experiment temperature was maintained at 27 °C for all NMR acquisition experiments.

Qualitative Interpretation of ^{31}P NMR Spectra. Publication data was processed using iNMR,[20] by Mestralab Research, running on Mac OSX. The fid files were Fourier transformed with 128 K zero-filling and a 0.5 Hz exponential line broadening factor. Phasing was performed manually between the IS region and each region of interest, to be integrated. Baseline subtraction was performed using a polynomial with 2 degrees of correction and 128 K filter. In addition to the spectral region of most interest (∼160−130 ppm) resonances were also observed to extend over the larger spectral region of between ∼190−0 ppm (Figure 2). The 2-Cl-TMDP signal appears at ∼175 ppm, downfield from the phosphitylated internal standard (TMDP-IS), aliphatic, phenolic, and carboxylic resonances. Immediately upfield from the region of interest is the resonance for the symmetrical anhydride of the 2-Cl-TMDP electrophile ((TMDP)$_2$O), formed from the reaction of 1 mol of water with 2 mols of 2-Cl-TMDP. All spectra were calibrated using this peak at 132.2 ppm. Two prominent unknown artifacts occur in the P(III) and P(V) regions of the spectra, upfield from the region of interest at 131.20 and 16.96 ppm, respectively. A publication by Hatzakis and Dais[21] has demonstrated that using similar reaction conditions to ours for the determination of the water content of olive oils, but in the absence of IL, one P(V) impuritiy is as a result of equilibrium tautomerisation of the typically unstable phosphorous acid cyclic diester (HOP(OR)$_2$), formed by reaction of the 2-Cl-TMDP with 1 mol of water, to a higher oxidation state phosphinic acid cyclic diester (HP(O)(OR)$_2$). This can be characterized by a large coupling

value observed for covalently bonded phosphorus and hydrogen, in the absence of any ^{1}H decoupling. It is also mentioned that a second artifact may be due to oxidation of the 2-Cl-TMDP phosphorus atom to the P(V) oxidation state phosphoryl chloride diester and that this and other potential artifacts in this region are highly dependent on the water content of the solution. The small intensity artifact, just upfield from the (TMDP)$_2$O, appears as a decomposition product over time. The formation appears to be slow, although in our case its formation was observed to be catalyzed by the presence of DMF. A compound exhibiting this resonance is also reported to be observed in a publication by Dayrit and de Vera et al.[22] although no explanation of its origin is given. When examined closer the broad peak, in comparison to (TMDP)$_2$O, resembles a doublet with a coupling value of 8.7 Hz. As the data is collected using the inverse gated decoupling technique, for the resolution of [1]H−[31]P couplings, while maintaining quantitative integrations, this value must be due to coupling with other nonidentical phosphorus nuclei in solution and is perhaps consistent with intermediate to long distance [31]P−[31]P coupling. Due to the possible presence of [31]P−[31]P coupling and close proximity of this artifact to the anhydride (TMDP)$_2$O resonance, this resonance is most likely occurring either via dioxaphospholane ring opening and subsequent oligomerization with free floating 2-Cl-TMDP or (TMDP)$_2$O electrophiles or as one-half of a symmetrical anhydride with a P(V) oxidation state acid. It is stressed by us and in the previous reports mentioned that the evidence, as proof of the true identity of these artifacts, is "tentative". This type of chemistry is typically complicated and out of the bounds of this publication on the understanding that the more reactive phosphite esters, such as those derived from 2-Cl-TMDP, are stable at moderate temperatures (<80 °C), in our observations. In addition, these artifacts are not expected to have any effect on the quantitative nature of our calculations, as they are observed to be formed in the absence of any biopolymer.

Quantitative Interpretation of ^{31}P NMR Spectra. All quantitative determinations of ^{31}P resonance integrations were carried out against the integration of a fixed amount of TMDP-IS, in solution. Inverse recovery experiments at the 90° pulse width for the lower molecular weight TMDP-IS resonance were recorded at each dilution under standard reaction conditions to determine the appropriate relaxation delay times (included in the Supporting Information). Approximately 2 s was generously added to these delay times to ensure complete relaxation. A correction factor had to be applied to quantitatively calculate the true P(V) resonance integrations due to a large decrease in excitation bandwidth observed, the further you go from the transmitter offset at 141 ppm. To achieve this, an excitation profile was carried out for the 90° pulse at variable ppm values from the transmitter offset. For each point, the integration values were normalized to a value of one and the corresponding correction factors determined by taking the reciprocal values (see Supporting Information). All P(III) resonances could be integrated as they were due to the minimal decrease in excitation bandwidth observed over the short ppm range, in comparison to the separation of the transmitter offset to the P(V) resonances.

Results and Discussion

Analysis Optimization and Solubility Issues. Initial optimization was performed on microcrystalline cellulose (MCC), as cellulose is the most abundant wood biopolymer and is highly insoluble in traditional nondestructive solvent systems. Predissolution of 5% w/w MCC in [amim]Cl at 80 °C for 18 h (to ensure complete dissolution) was followed by addition of excess reagents (Pyr and 2-Cl-TMDP), required for the theoretical maximum ^{31}P incorporation, based on total hydroxyls in cellulose (3/162 = 18.52 mmol/g). Minimal locking solvent (CDCl$_3$) was added and the data collected. Incorporation of ^{31}P nuclei was expected to occur as phosphite esters at the 2-, 3-, and 6- positions on cellulose (Scheme 1). A complete absence of any signals in the aliphatic phosphite ester region suggested that the phosphitylation reaction did not occur at all. The
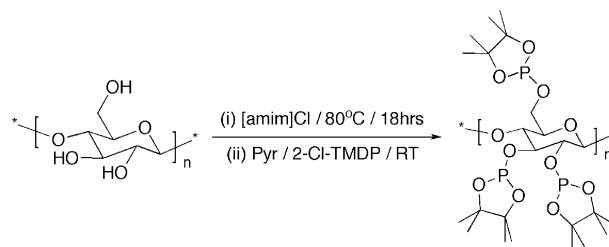
addition of 2-Cl-TMDP was accompanied by a phase separation and the TMDP-IS was observed as a sharp signal at 152.45 ppm, so it was assumed that the reaction had occurred to some unknown degree on the biopolymer. It was soon discovered that, by varying the quantity of locking solvent (CDCl$_3$) in the solution, a process of gradient dilution of the NMR mixture with a solution of Cr(acac)$_3$ in CDCl$_3$ (1 mg/mL) displayed different abundances of ^{31}P nuclei corresponding to the aliphatic phosphite esters of MCC. This involved addition of aliquots of 500 or 1000 μL to total additional CDCl$_3$ volumes of 500, 1000, 1500, 2000, 3000, and 4000 μL corresponding to CDCl$_3$ mol fractions of 0.49, 0.64, 0.73, 0.78, 0.84, and 0.87, respectively. Using this method, an increasing abundance of ^{31}P resonances in solution could be observed by increasing the hydrophobic component of the solvent system (see Supporting Information). This effect of solvent hydrophobicity was further demonstrated by dilution of the MCC reaction mixtures with DMF/CDCl$_3$ (1:4) solution. Using this more polar solution in place of CDCl$_3$, it was only possible to observe 30% of the total phosphite esters in solution at 4 mL dilution, only rising to 87% at 12 mL dilution, under the same reaction conditions (see Supporting Information). It is important to note here that the observed ^{31}P nuclei in solution are not representative of phosphitylation DS values but more likely to be a measure of the solubility of the partially or fully phosphitylated biopolymers in a given solvent mixture. This insolubility at low dilution and hydrophobicity is evident due to the observation of phase separation upon introduction of 2-Cl-TMDP into the reaction mixture. Further dilutions with CDCl$_3$ solution result in the formation of a clear gel, which eventually dissipates into the surrounding solution. Maximum degree of phosphitylation (DS with the phosphite ester) is assumed at this point for each dilution although definitive proof of this will be given later.

By using this process of gradient dilution for both MCC and EMAL samples, it was possible to arrive at maximized values for the total hydroxyl contents in solution phase by integrating the relevant functionality regions for each biopolymer (aliphatic, phenolic, or carboxylic) against TMDP-IS. These values, for maximum observed ^{31}P nuclei, corresponding to the total number of hydroxyls for each sample of known weight, were represented as observed ^{31}P nuceli (mmol/g) and plotted against mol fraction of CDCl$_3$ (Figure 3). Confirmation of the quantitative nature of the reaction at maximum dilution was possible by comparison of the maximum experimental value for total hydroxyls in MCC with the theoretical cellulose value (3/162 = 18.52 mmol/g). The EMAL value (ca. 6.28 mmol/g, 92.1% Klason content) was confirmed to be correct as the ^{31}P-biopolymer resonances maximized and maintained their value from lower mol fractions of CDCl$_3$ than for MCC (Figure 3). These values were also comparable to previous literature values for lignin in Norway Spruce EMAL.[4,5]

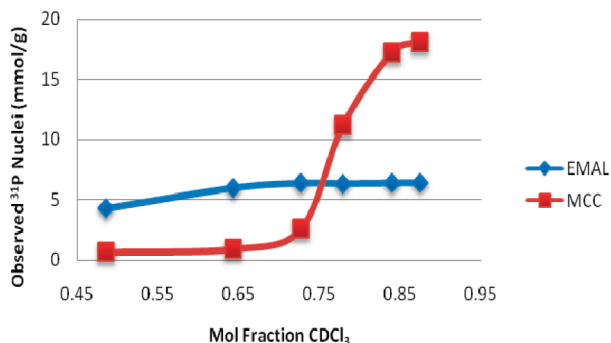One interesting examination can be made from Figure 3. The observed ^{31}P nuclei values (observed values in solution,

Figure 3. Observed ^{31}P nuclei during the gradient dilution of MCC and EMAL in [amim]Cl.
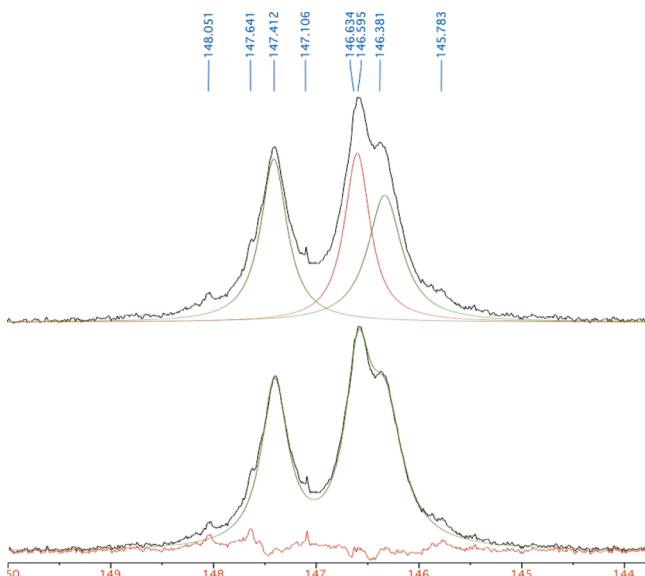

Figure 4. Deconvolution of ^{31}P-MCC spectra from [amim]Cl at 4 mL CDCl$_3$ dilution.

integrated against TMDP-IS) for the EMAL sample reach their maximum value at a much lower dilution than for the MCC sample. This is unusual in the respect that the hydrophilicity of lignin is expected to be much lower than for cellulose and is reflected in the total hydroxyl contents per weight unit of sample. Figure 3 suggests, however, that the fully phosphitylated samples of EMAL are solubilized at a lesser hydrophobicity than for the MCC samples. This can be rationalized by the fact that the methyl functionalities on the TMDP heterocycles effectively shield any partial charge bearing groups from large solvent molecules thus reducing the solvating ability of the polar ILs. With TMDP-functionalized lignin however, this effect is reduced. There is still significant potential for polar and $\pi-\pi$ interactions due to the irregular structure of lignin, in comparison to fully TMDP-functionalized cellulose. Altogether this provides for a more suitable environment for solvation by polar and aromatic imidazolium based ILs.

Qualitative Aspects of the [31]P Lignocellulose Spectra. Qualitative analysis of the MCC reaction for most dilution experiments shows two main resonances, one larger broad resonance at 146.5 ppm and one smaller at 147.4 ppm. All resonances are overlapping due to the high molecular weight of MCC (40500−48600 Da). Deconvolution of the spectra into three main resonances (146.38, 146.60, and 147.41 ppm) was straightforward, yielding low baseline residual error (Figure 4). Due to the overlap in these peaks and the complex combination of factors involved in predicting chemical shifts of ^{31}P reso-

nances, in comparison to ^{1}H NMR,[23] confident assignment of the deconvoluted resonances is troublesome and will not yield any valuable information within the scope of the present publication. As an example of the difficulty in predicting the resonances of ^{31}P nuclei, a publication by Ratier and Pouységu et al.[24] identified, with good confidence, the ^{31}P resonances of phosphite-labeled mono- and disaccharides using ^{31}P NMR INEPT spectroscopy, basing their effort on the earlier work of Archipov et al.[25] In this publication, the relative positioning of the C-2, C-3, and C-6 hydroxyl ^{31}P resonances are observed to change in an unpredictable manner, prohibiting any comparison to our deconvoluted spectra. The deconvolution however has identified several additional defined but broad residual resonances at 145.78, 147.64, and 148.05 ppm. As we have already determined that complete phosphitylation has occurred, these resonances are unlikely to arise from incomplete phosphitylation at one or more positions on the polysaccharide ring. This could provide reduced steric interaction causing a change in shielding in one or more of the nuclei. It is also unlikely that one or more of these residual peaks are as a result of phosphitylation of polymer chain end groups as a DP of 250−300 for this MCC sample provides too low an abundance of these end groups. Instead, it is more likely that a few recurring stable conformational changes have occurred in the already sterically hindered polymer backbone. Due to the steric hindrance imparted by the TMDP substituents, one or more of the ^{31}P nuclei associated with this local low energy conformation may be visible as separate resonances due to the change in steric environment around those nuclei.

The spectra for EMAL are more complicated containing broad resonances thoroughly assigned under the traditional molecular solvent conditions by Argyropoulos et al.[6] These assignments are for the most abundant functionalities such as aliphatic, syringyl phenolic, condensed phenolic, guiacyl phenolic, *p*-hydroxyl phenolic and carboxylic acids, after labeling with 2-Cl-TMDP. A comparison of the standard traditional molecular solvent method, was performed by the authors, with the new conditions based on [amim]Cl predissolution and dilution to an additional CDCl$_3$ solution content of 2 mL (see Supporting Information). Integration of the total biopolymer hydroxyl region for each method provides similar values for total hydroxyls in EMAL with the traditional Pyr/CDCl$_3$ based method giving 6.33 mmol/g (92.1% Klason) and the IL method giving 6.28 mmol/g (92.1% Klason). Qualitative comparison shows little difference in the aliphatic and phenolic regions, with the possible exception of one small resonance in the condensed region at 143.4 ppm and a slight increase in the *p*-hydroxyphenyl integrations at 138.0 ppm. The carboxylic acid region, however, visibly shows more variation in resonances, albeit in small abundances. These additional resonances do not appear as sharp signals, indicating high molecular weight, and may arise from the increased nucelophilicity of the chloride anion in the IL catalyzing the partial saponification of esters or unstable ethers into their constituent acids and alcohols. The most noticeable difference between the spectra is in the chemical shift of the TMDP-IS resonance. The IL method gives a 0.5 ppm downfield shift from the traditional method. The exact reason for this shift is unknown due to the complexity in predicting ^{31}P chemical shifts; however, Argyropoulos et al.[26] reported small changes in the chemical shifts of low molecular weight phosphitylated lignin model compounds upon varying quaternary ammonium salt and model compound concentrations in CDCl$_3$. They go on to report that the resonance maxima for higher molecular weight lignins were not dependent on these solvent conditions. This is consistent
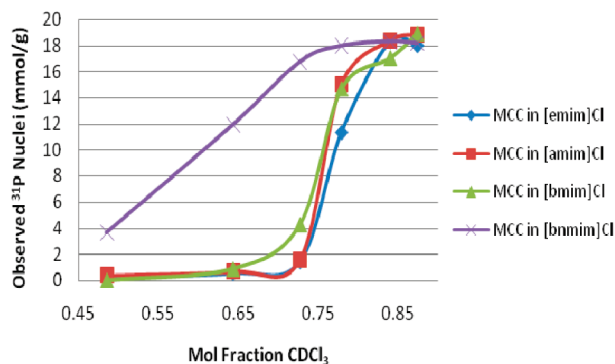
Figure 5. Observed ^{31}P nuclei during the gradient dilution of MCC in different ILs.

with our observations comparing the two methods and as such is no cause for concern in the chemical shift assignment of lignocellulosic biopolymers.

Ionic Liquid-Specific Effects. Armed with the knowledge that by varying the solvent hydrophobicity we can affect the observed abundance of MCC-phosphite esters, it was decided to examine the reaction with different ILs bearing different substituents that impart varying degrees of hydrophobicities (van der Waals content). The same reaction conditions, as for [amim]Cl, were examined with 5% MCC w/w in [emim]Cl, [bmim]Cl, and [bnmim]Cl. Dissolution rates were comparable with [amim]Cl, visually providing the fastest rate of dissolution and [bnmim]Cl the slowest over a 3 h time frame for both ILs. This could be due to the higher chloride content (H-bond breaking capability) of [amim]Cl (22.4% w/w) compared to [bnmim]Cl (17.0% w/w) although is more likely due to the lower viscosity of [amim]Cl at that temperature allowing for higher mass transfer. The reaction was performed as per the [amim]Cl experiment. The data was collected, processed, and plotted with the MCC [amim]Cl data, for comparison (Figure 5). All samples were observed to reach the maximum phosphitylation value of 18.52 mmol/g. The data shows strong similarities between [emim]Cl, [amim]Cl, and [bmim]Cl with the sharp onset of any significant abundance of MCC-phosphite esters occurring at a value of 0.75 for mol fraction of CDCl$_3$. At this point for these three ILs, the observed abundance of MCC-phosphite esters is between 6−10 mmol/g (32−54% of maximum phosphitylation). As a crude measure of relative IL hydrophobicity, the chloride content of pure [bmim]Cl (20.3% w/w) in comparison to pure [emim]Cl (24.2% w/w) and [amim]Cl (22.4% w/w), at higher concentrations of salt, should provide an environment more suited to the solubilization of hydrophobic compounds. At a CDCl$_3$ mol fraction of between 0.65−0.7 the observed appearance of ^{31}P resonances is more apparent for [bmim]Cl than for the more polar ILs. This is dramatically more pronounced for [bnmim]Cl with a chloride content of 17.0% w/w. [bnmim]Cl is the only IL in this series that exhibits the appearance of ^{31}P resonances with the lowest experimentally recordable mol fractions of CDCl$_3$ (0.5). This corresponds to the first addition of 500 µL of the CDCl$_3$ solution into the reaction mixture. To achieve almost maximum abundance of MCC-phosphite esters, the [bnmim]Cl sample requires the addition of 2 mL of additional CDCl$_3$ solution, while the remaining ILs required 3−4 mL. These results at this stage are a strong indication that the media hydrophobicity has a large part to play in the outcome of the reaction with respect to solubilization and homogenization. This is not unique to ILs, but under heterogeneous reaction conditions, the relative hydrophobicity of the IL may have a large impact on the DS and homogeneity of the final product.

In regard to cellulose functionalization, the room temperature viscosity of the IL is thought not to play a big part in this reaction due to the higher observed abundance of ^{31}P nuceli in the more viscous [bnmim]Cl, at the early stages of dilution, although this may be partly due to the high reactivity of 2-Cl-TMDP. The effect of viscosity may be more pronounced for lesser reactive electrophiles in pure ILs. This effect will also be enhanced on plant scale processes, at the same temperature, resulting in lower DS values and a reduction in homogeneity of the final product. From a practical point of view, in regard to the development of a robust analytical method, [amim]Cl provided the most manageable solution due to its low viscosity liquid state, incomparison to the other ILs. This meant that it was possible to seal the IL in a flask with a rubber septum to keep it dry, to be dispensed via a wide bore needle and syringe. It is important to also note, however, that the increased relative hydrophobicty of the [bnmim]Cl may allow for more concentrated lignocellulose solutions because the requirement for CDCl$_3$, to induce solubilization, is considerably reduced. Overall, in [bnmim]Cl, it may be that more biopolymer will be dissolved and fully functionalized with less CDCl$_3$ dilution, allowing for improved signal-to-noise ratios. Aliquots for the analytical process using [amim]Cl were removed using a wide bore needle and syringe to a fixed volume at room temperature. This was impossible with [bnmim]Cl, as the only other room temperature IL in the series, due to its high viscosity. [emim]Cl, [bnmim]Cl, and [bmim]Cl all required weighing of the thick glass or solid samples, allowing for uptake of water. This source of error may be removed by heating the samples above 80 °C, where all samples are liquid and the viscosities are considerably reduced, especially in the case of [bnmim]Cl.

Reaction Course. As mentioned previously, although the apparent observation of ^{31}P resonances seems to be dependent on the overall solvent hydrophobicity, this is no indication that the observed nuclei, from the quantification of solution phase ^{31}P-biopolymer resonances against the TMDP-IS, is representative of the actual DS value for those dilutions. From visual inspection of the reaction mixtures we already know that phase separation occurs with the early dilutions. It is expected that the addition of the highly reactive 2-Cl-TMDP reagent will react with all available nucelophiles at an early stage although this is not guaranteed. In an effort to determine the actual DS values for each dilution, the total quantity of observed ^{31}P nuclei, in solution, was integrated for each dilution, with correction of P(V) region integrations for decrease in excitation bandwidth. These values were then subtracted from the maximum observed phosphitylation quantities for each IL, at the highest mol fractions of CDCl$_3$, to give the total unobserved ^{31}P nuclei for each IL and each dilution (see Supporting Information), that is, quantification of any solid or gel state ^{31}P nuclei that cannot be directly observed using this solution phase technique. These values correspond to any ^{31}P nuclei covalently attached to the MCC hydroxyls, if any. The real value of these data points becomes apparent when you combine them with the previous observed ^{31}P nuclei values, for each dilution and each IL, to give an approximate value of the total incorporated (covalently bonded) ^{31}P nuclei in solid, gel and solution phase (Figure 6). Although the data in Figure 6 shows significant error due to the high dilutions and low numbers of transients collected, linear line fits for each IL clearly show a consistent incorporation of ^{31}P nuclei to MCC approximately equal to the theoretical total number of hydroxyls in cellulose (18.52 mmol/g). This conclusively tells us that the reaction is complete from the first addition of CDCl$_3$ solution to the last and that the apparent
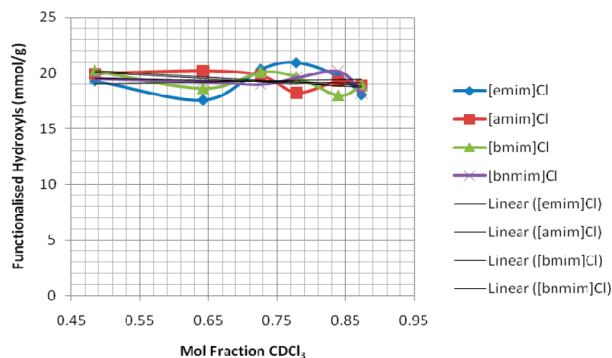
Figure 6. Total incorporated ^{31}P nuclei to MCC during the gradient dilution in different ILs.

change in observed hydroxyl resonances, in Figure 4, are solely due to the solubilization of the phosphitylated biopolymer, as the hydrophobicity of the media increases. This is consistent with the fact that there is no apparent change in selectivity for the two main resonance peaks shown for each dilution (see Supporting Information). What is not apparent is the DS value for the TMDP moiety directly after its introduction, before the addition of any CDCl₃ solutions, although due to the observation of phase separation and the high reactivity of 2-Cl-TMDP, significant incorporation of TMDP moieties is assumed under heterogeneous conditions. The actual DS of TMDP moieties at this stage is not determinable by solution phase ^{31}P NMR, preventing a comparison of the relative hydrophobic effects contributed by the IL anions on the DS and homogeneity of the reaction product under cosolvent free conditions.

Conclusions

It has been demonstrated that complete dissolution of both lignin (EMAL) and microcrystalline cellulose (MCC) is possible, into a range of chloride-based ILs of varying hydrophobicity. Dissolution of MCC was effective into all ILs examined at moderate temperature. Complete phosphitylation of all hydroxyls with tetramethyl-1,3,2-dioxaphospholanyl moieties in these samples was observable by determining the appropriate solvent conditions required to solubilize the fully phosphitylated biopolymers. The hydrophobicity of the cations on the different ILs were found to influence the solubility of the phosphitylated cellulose due to its ordered and hindered hydrophobic structure. The phosphitylated lignin, however, due to its irregular structure and potential for many different kinds of bonding interaction, was solubilized to a greater degree in the less hydrophobic mixtures, in comparison to the equivalent cellulose sample. This fractionation highlights the potential for the development of task specific ILs for the bioprocessing of lignocellulosic materials.

Supporting Information Available. ^{1}H NMR of ILs synthesized in this publication; Figure showing change in abundances of ^{31}P MCC-phosphite ester resonances with increasing CDCl₃ dilution; Graph showing the comparative dissolution of MCC-phosphite esters in DMF/CDCl₃ and CDCl₃ solutions; Graph showing the ^{31}P transmitter offset excitation profile (0 − 190 ppm) and correction factors for a 90° pulse angle and standard reaction conditions; Figure showing a comparison of the ^{31}P spectra of EMAL with the traditional and IL method; Graph showing the total unobserved ^{31}P nuclei for each IL and each dilution. This material is available free of charge via the Internet at http://pubs.acs.org.

References and Notes

(1) Klemm, D. Philipp, B. Heinze, T. Heinze, U. Wagenknecht; W. *Comprehensive Cellulose Chemistry: Volume 1, Properties of Cellulose*; Wiley-VCH: New York, 1998.
(2) Alén, R.; Holmbom, B.; Steinus, P. *Forest Products Chemistry*; TAPPI Press: Norcross, GA, 2000.
(3) Guerra, A.; Filpponen, I.; Lucia, L. A.; Argyropoulos, D. S. *J. Agric. Food Chem.* **2006**, *26*, 9696–9705.
(4) Guerra, A.; Filpponen, I.; Lucia, L. A.; Saquing, C.; Baumberger, S.; Argyropoulos, D. S. *J. Agric. Food Chem.* **2006**, *54*, 5939–5947.
(5) Argyropoulos, D. S. *J. Wood Chem. Technol.* **1994**, *1*, 45–63.
(6) Granata, A.; Argyropoulos, D. S. *J. Agric. Food Chem.* **1995**, *43*, 1538–1544.
(7) Crestini, C.; Argyropoulos, D. S. *J. Agric. Food Chem.* **1997**, *45*, 1212.
(8) Lu, F.; Ralph, J. *Plant J.* **2003**, *4*, 535–544.
(9) Kohler, S.; Heinze, T. *Macromol. Biosci.* **2007**, *3*, 307–314.
(10) Bloxam, A. G. GB Patent 359249, 1931.
(11) Swatloski, R. P.; Spear, S. K.; Holbrey, J. D.; Rogers, R. D. *J. Am. Chem. Soc.* **2002**, *18*, 4974–4975.
(12) Granström, M.; Kavakka, J.; King, A. W. T.; Majoinen, J.; Mäkelä, V.; Helaja, J.; Hietala, S.; Virtanen, T.; Maunu, S.; Argyropoulos, D. S.; Kilpeläinen, I. *Cellulose* **2008**, *3*, 481–488.
(13) Kilpeläinen, I.; Xie, H.; King, A. W. T.; Granstrom, M.; Heikkinen, S.; Argyropoulos, D. S. *J. Agric. Food Chem.* **2007**, *22*, 9142–9148.
(14) Xie, H.; King, A. W. T.; Kilpeläinen, I.; Granström, M.; Argyropoulos, D. S. *Biomacromolecules* **2007**, *12*, 3740–3748.
(15) Zhang, H.; Wu, J.; Zhang, J.; He, J. *Macromolecules* **2005**, *38*, 8272–8277.
(16) Mikkola, J.; Kirilin, A.; Tuuf, J.; Pranovich, A.; Holmbom, B.; Kustov, L. M.; Murzin, D. Y.; Salmi, T. *Green Chem.* **2007**, *11*, 1229–1237.
(17) Wu, J.; Zhang, J.; Zhang, H.; He, J.; Ren, Q.; Guo, M. *Biomacromolecules* **2004**, *2*, 266–268.
(18) Cao, Y.; Wu, J.; Meng, T.; Zhang, J.; He, J.; Li, H.; Zhang, Y. *Carbohydr. Polym.* **2007**, *4*, 665–672.
(19) Fukaya, Y.; Sugimoto, A.; Ohno, H. *Biomacromolecules* **2006**, *12*, 3295–3297.
(20) See http://www.inmr.net/.
(21) Hatzakis, E.; Dais, P. *J. Agric. Food Chem.* **2008**, *56*, 1866–1872.
(22) Dayrit, F. M.; Buenafe, O. E. M.; Chainani, E. T.; de Vera, I. M. S. *J. Agric. Food Chem.* **2008**, 5765–5769.
(23) Quin, L. D. 6.C. General trends and structural influences on shifts. In *A guide to organophosphorus chemistry*; Wiley-VCH: New York, 2000; pp 173−180.
(24) Pouységu, L.; De Jéso, B.; Lartigue, J. C.; Pétraud, M.; Ratier, M. *Magn. Reson. Chem.* **2000**, *8*, 668–674.
(25) Archipov, Y.; Argyropoulos, D. S.; Bolker, H. I.; Heitner, C. *Carbohydr. Res.* **1991**, *220*, 49–61.
(26) Argyropoulos, D. S.; Bolker, H. I.; Heitner, C.; Archipov, Y. *Holtzforschung* **1993**, *47*, 50–56.
(27) See http://www.ionicliquids-merck.de.

BM8010159